Tile Blockers as a Simple Motif to Control Self-Assembly: Kinetics and Thermodynamics

Constantine G. Evans
Hamilton Institute and Department of Computer Science, Maynooth University, Ireland

Angel Cervera Roldan
Hamilton Institute and Department of Computer Science, Maynooth University, Ireland

Trent Rogers
Hamilton Institute and Department of Computer Science, Maynooth University, Ireland
Computer Science & Computer Engineering, University of Arkansas, Fayetteville, AR, USA

Damien Woods
Hamilton Institute and Department of Computer Science, Maynooth University, Ireland

Abstract

A fundamental problem in crystallisation, and in molecular tile-based self-assembly in particular, is how to simultaneously control its two main constituent processes: seeded growth and spontaneous nucleation. Often, we desire out-of-equilibrium growth without spontaneous nucleation, which can be achieved through careful calibration of temperature, concentration and experimental time-scale a laborious and overly-sensitive approach. Another technique is to find alternative nucleation-resistant tile designs [Minev et al, 2001]. Rogers, Evans and Woods [In prep] propose *blockers*: short DNA strands designed to dynamically block DNA tile sides, altering self-assembly dynamics. Experiments showed independent and tunable control on nucleation and growth rates.

Here, we provide a theoretical explanation for these surprising results. We formally define the *kBlock* model where blockers bind to tiles at thermodynamic equilibrium in solution and stochastic kinetics allow self-assembly of a tiled structure. In an intentionally simplified mathematical setting we show that blockers permit reasonable seeded growth rates, akin to a non-blocked tile system at lower tile concentration, crucially giving nucleation rates that are exponentially suppressed. We then implement the kBlock model in a stochastic simulator, with results showing remarkable alignment with oversimplified theory. We provide evidence of blocker-induced tile buffering, where a large reservoir of blocked tiles slowly feeds a small unblocked tile subpopulation which acts like a regular, non-blocked, low tile concentration system, yet is capable of long-term buffered assembly. Finally, and perhaps most satisfyingly, theory and simulations align remarkably well with DNA self-assembly experiments over a wide range of concentrations and temperatures, matching the size of growth temperature windows to within 12%. Blockers are a straightforward solution to the challenging problem of simultaneously and independently controlling growth and nucleation, using a motif compatible with many DNA tile systems.

2012 ACM Subject Classification Applied computing → Chemistry; Applied computing → Physics; Theory of computation → Models of computation

Keywords and phrases Self-assembly, kinetic model, kinetic simulation, thermodynamic prediction

Digital Object Identifier 10.4230/LIPIcs.DNA.31.7

Supplementary Material *Collection (Data, code, and source)*: `https://doi.org/10.5281/zenodo.15272400`

Funding Supported by Science Foundation Ireland (SFI) under grants numbers 20/FFP-P/8843 and 18/ERCS/5746, European Research Council (ERC) under the European Union's (EU) Horizon 2020 research and innovation programme (grant No 772766, Active-DNA project), and European Innovation Council and SMEs Executive Agency (EISMEA), No 101115422, DISCO project. Views and opinions expressed are however those of the author(s) only and do not necessarily reflect those of the EU, ERC, EISMEA or SFI. Neither the EU nor the granting authority can be held responsible for them.

Acknowledgements We thank Erik Winfree for questions seeking a theoretical explanation of our experimental results at DNA28, as well as David Doty for suggesting, and Rebecca Schulman for discussions on, tile-buffering [20].

1 Introduction

Favourable self-assembly conditions typically catalyse two processes: continued growth of existing structures by monomer attachment, and spontaneous nucleation of new structures from free monomers in solution. Researchers usually prefer to have these two processes be at well-controlled and independent rates, a feat that can be incredibly difficult to achieve in practice. For example, perfect seeded growth [2, 21, 6, 26] requires no spontaneous nucleation but positive growth rate from a seed structure. Yet fabrication of seedless structures [23, 13, 10] requires a non-zero, ideally slow, rate of spontaneous nucleation, while having slow enough growth to avoid monomer depletion before structures complete. In almost all cases, we want to avoid low-temperature spurious growth. Thus, a fundamental problem for tile-based self-assembly is how to control both growth and nucleation rates for arbitrary tile-based systems.

A central principle of tile-based molecular self-assembly is that as temperature decreases, bonds strengthen, and so growth and nucleation should ordinarily become more favourable. This simple relationship allows systems to undergo controlled growth, for example, to create conditions where attachments by b bonds are favourable, while attachments by $b-1$ bonds are not. The control of the number of bonds required for favourable attachment allows for the computational power of algorithmic self-assembly, and is so closely linked to temperature that abstract models of tile assembly often use "temperature" to refer to the number of bonds required for attachment [24, 16]. Clean growth conditions with good bond specificity also seem important for good yield of uniquely addressed and periodic tile-based DNA nanostructures, exemplified by the use of slow anneals or long holding times at specific temperature, usually just below the lattice melting temperature [23, 10].

Growth from a pre-assembled seed structure of some form allows for some control of nucleation, and, sufficiently close to the melting temperature, "zig-zag" tile systems allow for an exponential reduction in spontaneous nucleation rates with increasing assembly width [22, 21]. However, these systems are inherently limited by nucleation pathways through increasing-size assemblies of tiles attaching purely by single-strength bonds, and must be close to the system's melting temperature to avoid those pathways becoming significant. This practically creates a temperature window for seeded growth, above the temperature where spontaneous nucleation is significant, but sufficiently below the melting temperature so that growth is significant on experimental timescales. The window can be quite small and difficult to widen: Woods, Doty et al. [26] found a seeded growth window of $<0.5\,^{\circ}\mathrm{C}$, increasing to $2.5\,^{\circ}\mathrm{C}$ only with a ten-fold reduction in concentration and corresponding decrease in growth rates.

A more dramatic approach to reducing spontaneous nucleation is to increase the difference in the number of bonds formed between a monomer and a growing assembly compared to between two monomers: from the 2 vs. 1 of usual threshold-2 systems, to k vs. 1. Minev et al. [15], and later Wintersinger et al. [25], showed that criss-crossing multi-bond tile motifs binding to several other tiles in a growing assembly, rather than only two, strongly reduced spontaneous nucleation across a broad range of temperatures. However, the technique may require further characterisation [15] or use of large DNA origami rods [25, 5]. And theoretically, even if the temperature window is much wider, at sufficiently low temperatures, the system must still allow for spontaneous nucleation, even if to a disordered assembly: one-bond attachments and nucleation pathways of some sort will eventually become favourable.

Rogers, Evans and Woods [17, 18] recently demonstrated a third approach, adding additional "blocker" strands, each complementary to individual glue domains on tiles, as shown in Figure 1. While binding weakly at growth temperatures, the transitory binding of the higher-concentration blockers to tiles, both in solution and on assemblies, was conjectured to interfere with tile attachment, reducing both growth and spontaneous nucleation rates, but hopefully, reducing nucleation rates, reliant on pathways with many one-bond attachments, more than two-bond growth. Experimental results were promising, showing that for some choices of blocker concentration, it is possible to have a system with seeded growth across a range of temperatures and no significant spontaneous nucleation at *any* temperature. However, the mechanism by which these effects were achieved remained unclear, lacking a theoretical basis beyond conjecture.

Contribution and paper structure

In Section 2, we define the kBlock kinetic model of tile assembly with blockers with the goal of explaining the results of Rogers et al. [17, 18]. In Section 3 we give two results. First, in Theorem 15, we show that behaviour of the kBlock model at a fixed temperature is largely equivalent to that of the kinetic Tile Assembly Model [24, 9] (kTAM) with a lowered, *effective tile concentration* and at the initial stages of growth before tile depletion dominates the kinetics. This effective tile concentration is dependent both on blocker concentration and temperature. Our second result, Theorem 19, is that with sufficient blocker concentration, the effective tile concentration decreases with decreasing temperature by enough to prevent spontaneous nucleation from ever becoming significant. Growth, meanwhile, can be confined to a temperature window of controllable width, with no significant growth, either seeded or by spontaneous nucleation, above or below the window (Remarks 16 and 17). And by increasing both tile and blocker concentrations, a "buffering" effect can be produced: for the same initial growth rate, the system with modified concentrations can incorporate far more tiles into assemblies before tile depletion prohibits further growth (Remark 18). Figures 2 and 4 illustrate these findings.

In Section 4, we show that this theoretical analysis fits well with kinetic model simulations for both growth and nucleation, and that simulations closely fit experimental results: for multiple experimentally-implemented systems, we show that temperature windows and relative growth rates with varying temperature can be closely matched by simulations using only tile and blocker concentrations, nearest-neighbour energies of glues, and a single lattice free energy parameter taken from the kTAM literature [10]. Finally, in Section 5 we draw several conclusions and suggest directions for future work.

2 kBlock model

Intuition behind the kBlock model

We construct our kBlock model of tile assembly with blockers by starting with the same assumptions as the kTAM [24, 9] for tile-assembly interactions, and then adding blocker-assembly and blocker-tile interactions. Intuitively, we will assume that blockers behave like tiles, but rather than taking a place in the lattice (assembly), they simply block a particular edge of the free (in solution) tile or free edge of an assembly-bound tile where they bind, and that blocked tile-edges are unavailable for tile binding. However, unlike the kTAM, where there is an assumption of operating in the limit of low assembly concentrations and hence all reactions can be approximated as taking place with constant tile concentrations, in

the blockers model, even disregarding assemblies entirely, tiles and blockers will interact in solution, since the concentrations involved may make those interactions significant. Rather than considering the kinetics of those interactions, since tile and blocker concentrations will generally be much higher than those of assemblies, we will assume that the concentrations of *free blockers* (not bound to a tile or assembly), and free *tile states* – each specific tile-blocker complex configuration – remain at the equilibrium concentrations they would reach in the absence of any assemblies. Then, these concentrations will be the concentrations for tile states and free blockers when considering attachment to assemblies.

2.1 kBlock model definitions

We let $\mathbb{R}, \mathbb{R}^+, \mathbb{R}^-$, respectively denote the real numbers, non-negative real numbers and non-positive real numbers (i.e. all three include 0). We use the notation $[x]$ to denote the number of instances of any object x in a fixed volume V, the *concentration*, where $[x] \in \mathbb{R}^+$. Σ denotes a finite alphabet, and Σ^* is the set of all strings over Σ. Throughout this paper, T is temperature, and we use $\beta = 1/(RT)$ for brevity, where R is the molar gas constant. Free energy always refers to Gibbs free energy.

▶ **Definition 1** (Tile type, Blocker)**.** A tile type $t = (l, E)$, or simply tile, is a square with a string label $l \in \Sigma^*$ over alphabet Σ, and 4 unit length edges each of which is a pair $e = (d, g) \in E$ where $d \in \{\text{N, E, S, W}\}$ is a direction and $g \in \Sigma^*$ is a glue name/type. Each glue g has a complement, denoted g^*. A blocker $\mathfrak{b}$ is a pair of the form $\mathfrak{b} = (d, g^*)$. No two blockers have complementary glues.

▶ **Definition 2** (kBlock instance)**.** An instance $\mathcal{B}$ of the kBlock model consists of a set of tiles $\mathcal{T}$ and blockers $\mathfrak{B}$, each $t \in \mathcal{T}$ and $\mathfrak{b} \in \mathfrak{B}$ having an associated non-negative real-valued *total species concentration* respectively denoted $c_\mathfrak{t}, c_\mathfrak{b} \in \mathbb{R}^+$. The system has a function $\Delta G_{\text{bond}} : \Sigma^* \times \mathbb{R}^+ \to \mathbb{R}$ such that $\Delta G_{\text{bond}}(g, T)$ is the free energy of glue g bound to its complement g^* at temperature T.

▶ **Definition 3** (Tile state)**.** A tile state is an instance (copy) of a tile type t, with 0 to 4 blockers, each bound to an edge. A blocker $\mathfrak{b} = (d, g)$ may bind only to edge $e = (d, g^*)$, i.e. if directions match and glues are complementary. We write $t\mathfrak{b}$ to denote a tile-blocker bonded complex. The *available edges* of a tile state do not have a blocker bound to them.

2.1.1 Tile states and blockers in solution bind together at equilibrium concentrations

In the remainder of this section we define the kBlock model as having two parts: (1) free blockers and tile states *in solution* at equilibrium concentrations as a function of their initial concentration and temperature, remaining unchanged during assembly, and (2) an assembly that grows by attachments of tile states and blockers via stochastic interactions; the tile states and blockers on an assembly are not required to be at solution equilibrium concentrations.

Hence, the kBlock model is "powered" [22]: individual events do not change blocker or tile state concentrations. That is, we take the limit of large volume so that removal or addition of individual blockers or tile states does not change their concentrations. Depletion effects can be approximated by changing the concentration parameters in the model.

▶ **Definition 4** (Tile states in solution)**.** The *solution* is a set of pairs of (s, c) where s is a blocker or tile state and $c \in \mathbb{R}^+$ is its concentration. For an edge of a tile type e and a temperature T, we let $p_\text{a}(T, e) \in [0, 1] \subseteq \mathbb{R}$, *the available edge probability*, be the probability that the edge is available (unblocked) in solution at equilibrium. We simply write p_a when T and e are clear from the context.

Although we defined notation for probabilities and concentrations, we have not yet given them explicit values. In Remark 6 those come from chemical equilibrium, and a lemma:

▶ **Lemma 5.** *The concentration of unbound tile states of a tile type t with a particular edge available is $p_a c_t$, and the concentration of unbound blocker instances of a blocker $\mathfrak{b}$ is $[\mathfrak{b}] = c_\mathfrak{b} - p_a C_t$, where $C_t = \sum_{t'} n_{t',\mathfrak{b}}\, c_{t'}$ is the sum of the concentrations of all tiles with $n_{t',\mathfrak{b}} > 0$ glues complementary to the blocker $\mathfrak{b}$.*

Proof. By Definitions 2 and 4 (initial tile concentration c_t and available edge probability p_a), we get the first conclusion ($p_\mathrm{a} c_\mathrm{t}$). The second comes from conservation of mass. ◀

▶ Remark 6 (Equilibrium concentrations of tiles and blockers). Practically, $p_\mathrm{a}(T, e)$, written here as a function of temperature T and edge identity e, can be determined by the equilibrium concentrations of tiles and blockers in isolation in solution, ignoring assemblies. While the system may have many tile types and blockers, reactions involving each blocker are independent and can be considered in isolation. By standard chemical reaction thermodynamics in solution [14, 3], we define an abstract reaction coordinate $\xi_{i,\mathfrak{b}}$ for each reaction $t_i + \mathfrak{b} \rightleftarrows t_i\mathfrak{b}$. Then, the change in free energy G with each reaction is

$$\frac{\mathrm{d}G}{\mathrm{d}\xi_{i,\mathfrak{b}}} = (RT \ln[t_i\mathfrak{b}] - RT \ln[t_i] - RT \ln[\mathfrak{b}] + \Delta G_\mathrm{bond}(T)) \tag{1}$$

G has a minimum where, for each tile-blocker pair, $\frac{\mathrm{d}G}{\mathrm{d}\xi_{i,\mathfrak{b}}} = 0$ [3], implying equilibrium concentrations $[t_i\mathfrak{b}] = [t_i][\mathfrak{b}]e^{-\beta\Delta G_\mathrm{bond}(T)}$. By conservation of mass $[t_i] + [t_i\mathfrak{b}] = c_\mathrm{t}$, hence

$$[t_i] = \frac{c_\mathrm{t}}{1 + [\mathfrak{b}]e^{-\beta\Delta G_\mathrm{bond}(T)}} \qquad p_\mathrm{a} = \frac{1}{1 + [\mathfrak{b}]e^{-\beta\Delta G_\mathrm{bond}(T)}} \tag{2}$$

We claim that p_a is a probability, in other words that $p_\mathrm{a} \in [0, 1] \subset \mathbb{R}$ as follows: without blockers $p_\mathrm{a} = 1$ for all temperatures T and ΔG_bond since $0 = [\mathfrak{b}] \leq c_\mathfrak{b}$, otherwise $0 < p_\mathrm{a} < 1$ for $[\mathfrak{b}] > 0$ and all T and ΔG_bond. Furthermore, the expression for p_a is in terms of $[\mathfrak{b}]$, the concentration of unbound blocker instances, rather than the total species concentration $c_\mathfrak{b}$ of the blocker $\mathfrak{b}$. In the limit where total blocker concentrations are large multiples of total tile concentrations, the concentration $[\mathfrak{b}]$ is close to $c_\mathfrak{b}$, and where noted we use that approximation: $[\mathfrak{b}] = c_\mathfrak{b}$. But more precisely, for all concentrations, the combination of conservation of mass constraints and equilibrium conditions results in the analytic solution

$$[\mathfrak{b}] = \frac{1}{2}\left(c_\mathfrak{b} - C_\mathrm{t} - e^{\beta\Delta G_\mathrm{bond}(T)} + \sqrt{\left(C_\mathrm{t} - c_\mathfrak{b} + e^{\beta\Delta G_\mathrm{bond}(T)}\right)^2 + 4c_\mathfrak{b}e^{\beta\Delta G_\mathrm{bond}(T)}}\right) \tag{3}$$

This has the effect, at low blocker concentrations relative to C_t, of increasing p_a. However, while our theoretical analyses and simulations use the precise value of $[\mathfrak{b}]$ in Equation (3) to calculate p_a, in this and related experimental work [17, 18] we focus on high concentration blockers, where depletion of unbound blockers is not significant, and the aforementioned $[\mathfrak{b}] = c_\mathfrak{b}$ approximation is sufficient. Figure 2(left) shows how close the approximation is.

2.1.2 Assembly reactions are stochastic

▶ **Definition 7** (Assembly)**.** An assembly of a kBlock system $\mathcal{B}$ is a function $\alpha : \mathbb{Z}^2 \to \mathcal{T}$ where the domain of α is connected in $\mathbb{Z}^2$ and where $\mathcal{T}$ is the set of all tile states of $\mathcal{B}$. Intuitively, an assembly is a connected lattice of tile states.

▶ **Definition 8** (kBlock dynamics and rates)**.** A single step $\alpha \to_1 \alpha'$ in the kBlock model maps one assembly α to another assembly α' where both differ by the attachment or detachment of a single tile state or blocker governed by four rate equations, illustrated in Figure 1:

$$r_{\mathrm{t,att}} = k_{\mathrm{f}}[t] \tag{4}$$

$$r_{\mathrm{t,det}} = k_{\mathrm{f}} e^{b\beta\Delta G_{\mathrm{bond}}(T) - (b-1)R\Delta S_{\mathrm{lat}}} \tag{5}$$

$$r_{\mathfrak{b},\mathrm{att}} = k_{\mathrm{f}}[\mathfrak{b}] = k_{\mathrm{f}}\left(c_{\mathfrak{b}} - p_{\mathrm{a}} C_{\mathrm{t}}\right) \tag{6}$$

$$r_{\mathfrak{b},\mathrm{det}} = k_{\mathrm{f}} e^{\beta\Delta G_{\mathrm{bond}}(T)} \tag{7}$$

These are applied and explained as follows:

1. Tile state attachment ($r_{\mathrm{t,att}}$): at every empty coordinate in $\mathbb{Z}^2$ adjoining at least one tile state in α, each tile state in solution may attach at the coordinate if (1) the tile state has at least one glue complementary to the glue on the adjoining tile state, (2) the tile state would not be adjacent to any edge of any tile state in α with a bound blocker, and (3) no edge of the tile state with a bound blocker would be adjacent to another tile state in α. The rate of attachment per tile state t satisfying the criteria is $r_{\mathrm{t,att}} = k_{\mathrm{f}}[t]$, where $[t]$ is the concentration of the tile state satisfying the criteria.
2. Tile state detachment ($r_{\mathrm{t,det}}$): any tile state in α may detach, if detaching does not result in the assembly becoming disconnected, at a rate of $r_{\mathrm{t,det}} = k_{\mathrm{f}} e^{b\beta\Delta G_{\mathrm{bond}}(T) - (b-1)R\Delta S_{\mathrm{lat}}}$, where b is the number of bonds between the tile state and adjoining tiles in α. ΔS_{lat} is defined as an entropic penalty for the formation of multiple bonds.
3. Blocker attachment ($r_{\mathfrak{b},\mathrm{att}}$): at every edge of every tile state in an assembly where no blocker is bound, there is no adjacent tile, and the system has a blocker complementary to the edge's glue, that blocker may attach to the edge with a rate of $k_{\mathrm{f}}[\mathfrak{b}] = k_{\mathrm{f}}\left(c_{\mathfrak{b}} - p_{\mathrm{a}} C_{\mathrm{t}}\right)$, where C_{t} is the sum of the total species concentrations of all tile types with a glue complementary to the blocker (Lemma 5).
4. Blocker detachment ($r_{\mathfrak{b},\mathrm{det}}$): at every edge of every tile state in an assembly that has a bound blocker, the blocker may detach from the edge with a rate of $k_{\mathrm{f}} e^{\beta\Delta G_{\mathrm{bond}}(T)}$.

▶ **Definition 9** (Seed)**.** The assembly α of a kBlock system prior to any step being taken is defined as the seed of the system. This serves as a starting point from which the system may grow. Growth is said to be unseeded if the seed is empty (i.e. $\mathrm{dom}(\alpha) = \emptyset$).

▶ Remark 10 (Why do we disallow attachment of partially blocked tiles?). These event definitions include the choice of disallowing tile state attachment if *any* blockers interfere. Including these attachments would seem more physically realistic. However, as the model treats tile and blocker attachments and detachments as elementary steps, rather than modeling individual bond formation and breakage, allowing partially blocked attachments would violate detailed balance. Much of the theoretical analysis of the kBlock model can be adapted to accommodate the extra events. However, we found that the temperature-dependent behaviour of the kBlock model fit experimental observations significantly better without partially blocked attachments. Although surprising, physically-plausible mechanisms could result in partially-blocked attachments being unlikely to result in stable tile attachment and thus make the model without partially blocked attachments more accurate. For example, there could be a small difference in blocker and single-bond tile free energies that would make blocker detachment less likely than tile detachment, and there could be a delay to forming an additional bond that would make a tile attached by a single bond more likely to detach before forming a second bond to a newly-available adjacent glue. We explore the two model choices further in Section B.

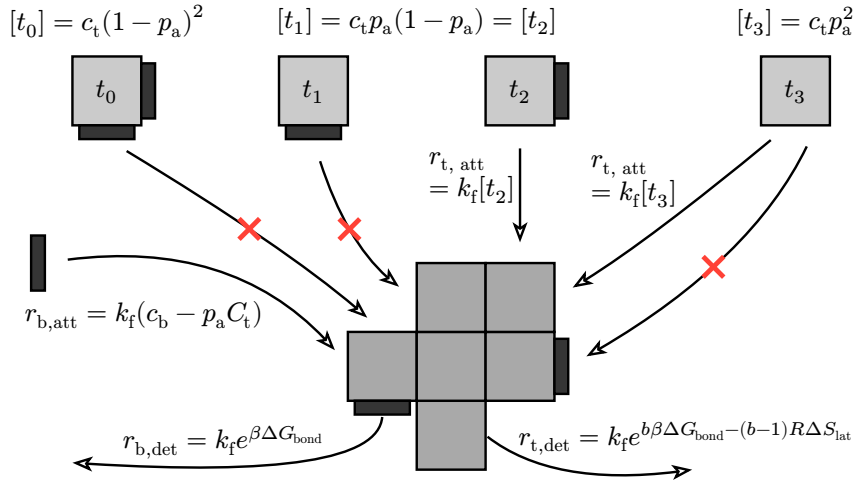

Figure 1 Summary of the kBlock model. **Top:** Blockers and tile states bind in solution and are held at a temperature-dependent equilibrium. **Centre:** Blockers and tile states stochastically attach to, or detach from, a dynamically growing/shrinking assembly (centre). Blockers may attach to any available matching glue on a tile on the assembly, while tiles can attach to any empty position where the tile can make at least one bond, and where there is no blocker between tiles; both blockers and tiles attach with the same forward rate constant, simply dependent on concentration. **Bottom:** Tile states and blockers detach based on bond free energy.

We assume that the lattice penalty ΔS_{lat}, used above, is entropic and proportional to the number of bonds made beyond one. This penalty was calculated in [10] as $\alpha = -7.12$, where α is a parameter in the unitless formulation of the kTAM (Section A), based on [11, 12]. This parameter is equivalent in our formulation to $-14.12\,\mathrm{cal\,mol^{-1}\,K^{-1}}$ for both SSTs and DX tiles; we do not expect that core tiles will significantly differ. The model as defined above excludes any detachment that would disconnect the assembly, as this would violate detailed balance; in practice, as with the kTAM, implementations may choose to include "fission" events, for example, by discarding one of the disconnected regions. While the model includes blocker attachment and detachment events on assemblies, for a given edge on an assembly that is not adjacent to another tile state, the blocker attachment and detachment rates result in the probability of that edge being available being $r_{\mathfrak{b},det}/(r_{\mathfrak{b},det} + r_{\mathfrak{b},att}) = 1/(1 + [\mathfrak{b}]e^{-\beta\Delta G_{bond}(T)})$, which is the same as p_a in Equation (2). This probability is useful in the theoretical analysis of Section 3.

2.2 kBlock$_2$: a simplified theoretical model for mathematical results

The kBlock and kTAM [24, 9] models are used for our computer-simulation-based results (Section 4). However, for mathematically derived results on growth rates in Section 3, we use two simpler models, called the kTAM$_2$ and kBlock$_2$, which we now justify.

Most tile systems of experimental interest have intended growth pathways primarily using two-bond attachments, and are grown at temperatures where two-bond attachments are slightly favourable. In the limit of low concentrations and slow growth slightly below the two-bond melting temperature where attachment and detachment by two bonds are equally favourable, one-bond attachments detach much faster than they attach (and are mainly of relevance to erroneous growth pathways), while three- and four-bond detachments are slow enough to be insignificant. Thus, we view two-bond tile attachment and detachment events as being most significant [9]. For ease of analysis, we define models constrained to two-bond attachment and a few other reasonable simplifications:

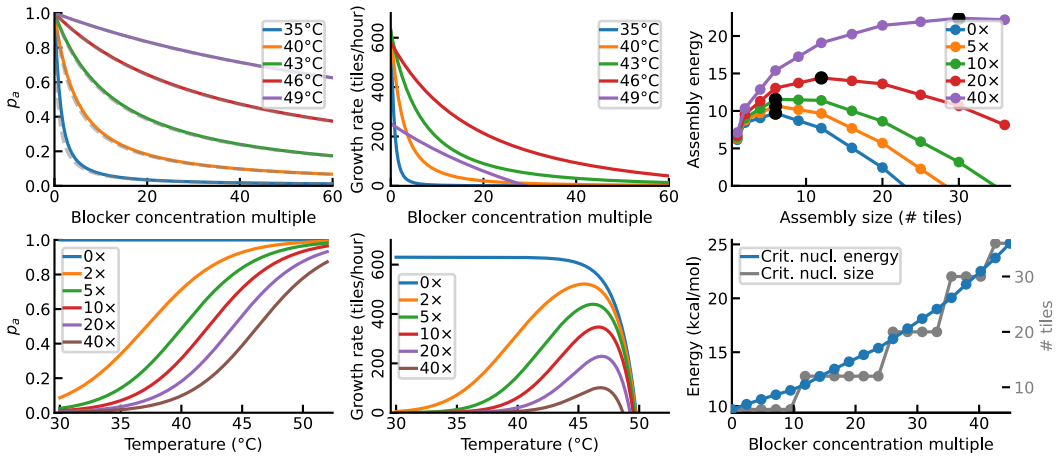

Figure 2 Plots derived from theoretical results in Sections 2.1.1 and 3. **Left**: The probability p_a of a tile side being unblocked, Equation (2), decreases with increasing blocker concentration and decreasing temperature. Solid curves: blocker concentration $[\mathfrak{b}]$ from Equation (3). Dashed: high-blocker-concentration approximation $[\mathfrak{b}] = c_\mathfrak{b}$, Remark 6. **Middle**: Two-bond growth rates (Section 3.1) increasing blocker concentration suppresses growth at low temperatures, and increasing detachment rates prohibits growth at high temperatures, creating a growth temperature window (bottom). **Right**: Nucleation (Section 3.2): increasing blocker concentrations increases assembly energies. Nucleation pathways go through a sequence of assemblies of increasing size and decreasing favourability, until a critical nucleus size is surpassed wherein growth is mostly favourable. Plots: critical nucleus size and free energy (unfavourability) increases with blocker concentration, with black dots in the top plot being critical nuclei.

▶ **Definition 11** (kTAM_2)**.** The kTAM_2 model is the kTAM [24, 9] restricted to only allow tile attachments by two bonds and detachments by two bonds, to have all bond strengths to be equal, and to have all tile concentrations to be equal (c_t).

▶ **Definition 12** (kBlock_2)**.** The kBlock_2 model is the kBlock restricted so that: (1) each tile type has at most two blockers, each for a distinct edge of the tile, and these blockers attach only to that tile; (2) every tile state attachment involves two bonds, each having either a blocker in the system for the glue on the attaching tile, or a blocker in the system for the glue on the adjoining tile; (3) all bond strengths are equal; and (4) all total tile concentrations are equal (c_t) and all total blocker concentrations are equal ($c_\mathfrak{b}$).

3 Theoretical analysis

In this section we prove some results for growth in the restricted kBlock_2 model (Definition 12), and nucleation in the kBlock_2 generalised to allow 1- and 2-bond attachments.

3.1 Growth rate in the kBlock_2 model

Theoretically modelling growth rates is challenging due to assemblies changing frontier size over time. Indeed for algorithmic systems it can be provably algorithmically hard, or even undecidable, to predict whether a single tile is placed at some location [16, 4]. Hence, we consider an intentionally oversimplified growth rate in our simplified kinetics models:

▶ **Definition 13** (Two-bond growth rate)**.** *In the $kTAM_2$ and $kBlock_2$, the two-bond growth rate is the average rate an assembly increases in size, via both attachments and detachments.*

In the kTAM$_2$, the two-bond growth rate for a system with an assembly growth front, or frontier, constant in size over time is $r_2 = \gamma \cdot (r_{\text{t,att}} - r_{\text{t,det}})$, where γ is a positive constant factor dependent on the shape of growth front [24, 9]. For example, $\gamma = 1$ for a "zig-zag" system [22] with frontier size 1. For frontier sizes that change over time, γ is a more complicated function, something we do not wish to explicitly handle here. In this subsection we seek a 2-bond growth rate result for the kBlock$_2$ model, in terms of the kTAM$_2$, and leaving γ as an undefined system-dependent function.

▶ **Lemma 14.** *For any kBlock$_2$ instance $\mathcal{B}$, at fixed temperature T, the available edge probability p_a (Equation (2)) is identical for every tile edge.*

Proof. By Equation (2), p_a is a function of (1) temperature – which is fixed, (2) glue free energy $\Delta G_{\text{bond}}(T)$ – which is equal for all glues. and (3) blocker concentration [$\mathfrak{b}$] – which is equal for all blockers in the system by analysis of Equation (3). ◀

▶ **Theorem 15** (Each kBlock$_2$ system has a corresponding kTAM$_2$ system)**.** *Let $\mathcal{B}$ be a kBlock$_2$ system with tile concentration $c_{\mathcal{B}}$, and let p_a be $\mathcal{B}$'s available edge probability (a single value for all edges by Lemma 14). There is a kTAM$_2$ system $\mathcal{K}$ with the same tile types, seed and tile attachment/detachment rate constants as $\mathcal{B}$, with tile concentration per tile type $c_{\mathcal{K}} = p_a^2 c_{\mathcal{B}}$ such that both systems have the same 2-bond growth rate. We call $c_{\mathcal{K}}$ the "effective tile concentration".*

Proof. By hypothesis, tile detachment rates for the kBlock$_2$ and kTAM$_2$ systems are the same. Tile attachments, however, will be influenced by blockers. In the kTAM$_2$ system, a potential tile attachment has rate $k_{\text{f}} c_{\mathcal{B}}$, where we use notation $c_{\mathcal{B}}$ or $c_{\mathcal{K}}$, depending on the system, instead of the usual c_{t}.

In the kBlock$_2$ system, for the same assembly position, the same attachment will require that no blockers are bound to the edges between the tile and adjoining tiles in the assembly. In the kBlock$_2$ model, there are exactly two blockers involved, and each may be complementary to either a glue on the attaching tile state, or a glue on a tile state in the assembly. If the blocker is complementary to a glue on the tile, then there is a p_{a} probability of a tile state that has that edge unbound, by the definition of p_{a} in Equation (2). If the blocker is complementary to a glue on the assembly, there is also probability p_{a} that the edge will be available at any given moment since the attachment and detachment rates satisfy the same equilibrium concentrations of blocker/no blocker for a single site.

As neither blocker can be present for attachment to be possible, there is a p_{a}^2 probability that, for a randomly chosen tile state from solution at a random moment, the attachment will be possible; this results in an attachment rate of $r_{\text{f},\mathcal{B}} = p_{\text{a}}^2 \cdot k_{\text{f}} c_{\mathcal{B}}$. The expression for the two-bond growth rate for a kTAM$_2$ or kBlock$_2$ system is of the same form $r_2 = \gamma\,(r_{\text{f}} - r_{\text{r},2})$: Since, by hypothesis, both systems have identical detachment rates $r_{\text{r},2}$, the 2-bond growth rate r_2 will be equal for both systems if the attachment rates r_{f} are equal for both systems. Setting the kTAM$_2$ tile concentration to $c_{\mathcal{K}} = p_{\text{a}}^2 c_{\mathcal{B}}$ gives exactly that since for $\mathcal{K}$, the attachment rate is $r_{\text{f},\mathcal{K}} = k_{\text{f}} c_{\mathcal{K}} = k_{\text{f}} p_{\text{a}}^2 c_{\mathcal{B}} = r_{\text{f},\mathcal{B}}$. ◀

▶ Remark 16 (Blocked growth at low temperature). A corollary of the previous theorem is that blockers completely kill low-temperature growth, which can be seen as follows. From Equation (2), the probability p_{a} that a side is available is inversely exponentially dependent on temperature. Higher blocker concentration also drives this probability down, albeit linearly. Hence, in the systems studied here, at low temperatures and high blocker concentration, p_{a} will tend to zero, and thus the 2-bond growth rate will also tend to zero (Figure 2 (middle-top)). By the same reasoning, and since every bond or its complement has a blocker,

the attachment rate for 1-bond growth, $k_f p_a c_{\mathcal{B}}$, will always be less than the detachment rate, $k_f e^{\beta \Delta G_{\text{bond}}(T)}$, so long as the unbound blocker concentration $[\mathfrak{b}]$ is greater than the tile concentration.In contrast, in regular unblocked systems growth simply happens below the melting temperature, and at low temperatures suffer from unintended structures likely created from 1-bond growth and nucleation [26] (Suppl. Info. A, Sect. S5.1).

▶ Remark 17 (Growth window). There is a temperature growth window: above the melting temperature the growth rate is less than zero, and, by Remark 16, at low temperatures the 2-bond growth rate tends to zero. In between these extremes, there is positive growth, as shown in Figure 2 (middle-bottom). The width of the 2-bond growth window is blocker concentration dependent, with more blockers resulting in a narrower window.

▶ Remark 18 (Buffering). Blockers also result in a "tile-buffering" effect [20], causing changes to the growth rate to be slower, as tiles are incorporated into assemblies, than the same system without blockers. Or, equivalently, as tiles are used, the effective tile concentration c_{eff} (defined in the statement of Theorem 15) changes more slowly than the concentration of tiles used. While the kBlock model does not account for concentration changes from tile attachment and detachment events, the effect of a certain concentration of tiles being incorporated into assemblies, and thus unavailable for attachment, can be examined by changing the concentrations in the model. Defining c_{used} as the concentration of tiles incorporated into assemblies at some point during growth, so remaining tile concentration is $c_t = c_t^{(\text{initial})} - c_{\text{used}}$, and from Section 3.1 letting r_2 be the 2-bond growth rate, it is easily seen that $\mathrm{d}r_2/\mathrm{d}c_{\text{used}} = -\gamma k_f p_a$, and $\mathrm{d}c_{\text{eff}}/\mathrm{d}c_{\text{used}} = -p_a$: if a particular concentration c_{used} of tiles is used, the effective concentration available for attachment is reduced only $p_a c_{\text{used}}$, rather than c_{used} as it would be without blockers. Practically, this means that, if a particular growth rate is desired, a system with blockers can use a larger total tile concentration, and incorporate more tiles with less effects from depletion. See Figure 4.

3.2 Nucleation rate in the kBlock model

Here, spontaneous nucleation from solution, or simply nucleation, refers to the self-assembly process whereby assemblies form in slightly supersaturated conditions, in other words just below the 2-bond crystal melting temperature. Nucleation rates are difficult to model due to multiple simultaneous pathways and geometric concerns. Schulman and Winfree [22] applied classical nucleation theory to derive a mathematical upper bound on the nucleation rate in DNA tile self-assembly. Close to the crystal melting temperature, nucleation pathways are unfavourable until some large enough assembly called a critical nucleus has assembled, from which growth is favourable. Their approach considers the assemblies visited along nucleation pathways to critical nuclei, observing that the most favourable of these, including any critical nucleus, can be used to derive an upperbound on the nucleation rate. The proof of the following theorem uses that upperbound [22]. The theorem is stated for a generalisation of the kBlock$_2$ that allows both 1- and 2-bond attachments (because nucleation is impossible if there are no 1-bond attachments), but more restricted than the kBlock to avoid complications of arbitrary combinations of blockers and concentrations. Also, using ideas from [22] we consider only the critical nucleus that is the most stable of all the critical nuclei, and that growth from it is favourable (by two-bond attachments).

▶ **Theorem 19.** *For a system in the kBlock with a critical nucleus of N tiles and B bonds, where every tile has exactly two blockers, attachments by one bond are not favourable, and every glue on the critical nucleus perimeter is required for continued growth, the classical nucleation theory upper bound [22] on the nucleation rate through that critical nucleus is reduced by $(p_a)^{2(N+1)}$ compared to the same system without blockers.*

Proof. We first define the free energy of an assembly α, in the kTAM [22]:

$$G(\alpha) = B\Delta G_{\text{bond}}(T) - T(B-N)\Delta S_{\text{lat}} - RT\sum_{t\in\alpha}\ln[t] \tag{8}$$

where $N = |\alpha|$ is the total number of tiles in assembly α, B is the total number of bonds in α, and each t is an instance (copy) of a tile in α, i.e. the sum has N terms.

Next, in Equation (9), we define the assembly free energy of a critical nucleus in the kBlock model (the version assumed by the theorem hypotheses) which is justified as follows. In the kBlock and kTAM, energetic contributions of bonds in the assembly are equal. However, in the kBlock, the tile concentration of tiles available to bind to an assembly is $p_{\text{a}}^2 c_{\text{t}}$: by assumption, each tile (with, as usual, initial unblocked concentration c_{t} and available edge probability p_{a}) has two blockers that bind to it and hence the completely unblocked tile state has concentration $p_{\text{a}}^2 c_{\text{t}}$ through the entire assembly process, which we substitute for $[t]$ in Equation (8), noting that the sum of logarithms in the assembly free energy $G(\alpha)$ allows these multiplicative terms to be separated in Equation (9). Also, in Equation (9) we ignore free energy contribution from blockers bound to the perimeter of the assembly, as by hypothesis only tile states without blocked edges on the perimeter of the assembly will allow for continued growth.

$$G(\alpha) = B\Delta G_{\text{bond}}(T) - T(B-N)\Delta S_{\text{lat}} - RTN\ln c_{\text{t}} - 2RTN\ln p_{\text{a}} \tag{9}$$

Given a particular critical nucleus α, as shown for the kTAM in similar conditions [22], we assume $[\alpha]$ at any time is bounded by the equilibrium concentration $[\alpha]_{\text{eq}} = \exp(-\beta G(\alpha))$. Thus, the nucleation rate through a pathway containing that critical nucleus is bounded from above by $r_{\text{cn}} = Fr_{\text{f}}\exp(-\beta G(\alpha))$, where r_{f} is the tile attachment rate for two-bond attachments and F is the number of two-bond attachment sites: in other words, the flux through the critical nucleus, ignoring reverse reactions and one-bond attachments (which, being unfavourable, would mean the α would not be the critical nucleus). Since two-bond attachments to the critical nucleus must involve two unblocked edges, the attachment rate is $k_{\text{f}}p_{\text{a}}^2 c_{\text{t}}$. The kBlock assembly free energy differs from the kTAM assembly free energy by $-2RTN\ln p_{\text{a}}$; this results in a change to the nucleation rate, via the $\exp(-\beta G(\alpha))$ term, of $\exp(-2\beta RTN\ln p_{\text{a}}) = p_{\text{a}}^{-2N}$. When combined with the additional p_{a}^2 from r_{f}, this results in r_{cn} being multiplied by $p_{\text{a}}^{2(N+1)}$ compared to the kTAM. ◀

It follows from the previous theorem and the definition of p_{a} that the nucleation rate, like the growth rate, will tend towards zero as temperature decreases when the blocker concentration is high, resulting in a temperature window where unseeded nucleation occurs.

4 Simulations and comparisons with experimental results

As an extension of the kTAM, the kBlock model is amenable to similar simulation techniques. We implemented the model as a Gillespie algorithm simulation in the Rgrow tile assembly simulator [8]. When sequences for glues are provided, Rgrow calculates the free energy for the glues based on the nearest-neighbor model using parameters from [19]; these were used for comparisons with experimentally-implemented systems. We consistently used a value of $\Delta S_{\text{lat}} = -14.12\,\text{cal}\,\text{mol}^{-1}\,\text{K}^{-1}$ for all simulations [10].

Experiments with blockers in Rogers et al. focused on systems forming periodic nanotubes, uniquely-addressed around the tube to force a minimum circumference of 12 helices, and using a DNA origami seed for seeded growth [17, 18]. Seeded tubes are particularly simple

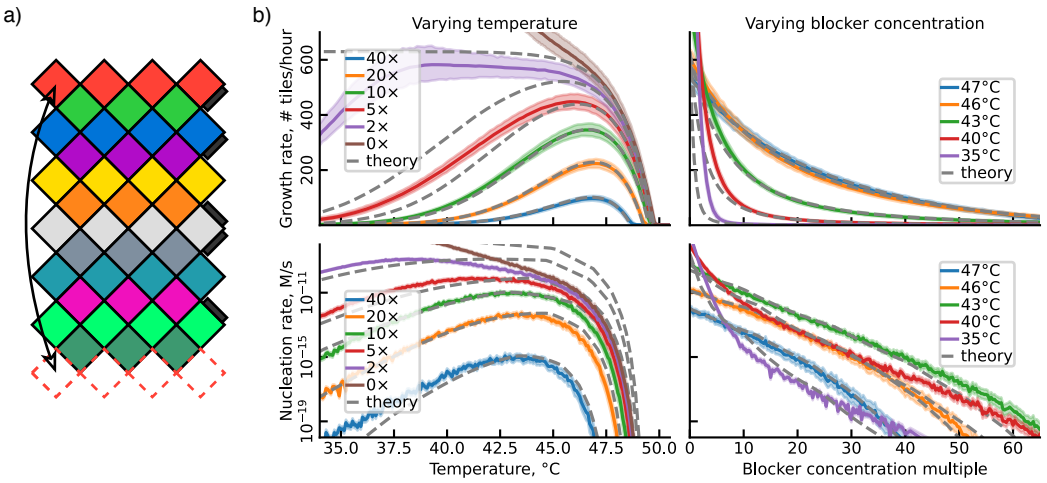

Figure 3 (a) A simple 12-tile tube system with blockers. (b) Plots showing both simulation (solid curves) and theory (dashed) for growth and nucleation rates: on the left, systems with different blocker concentrations as a function of temperature, and on the right, systems at different fixed temperatures as a function of blocker concentration. Growth rate simulations used 1,024 simulated seeded assemblies, each grown until reaching 1,200 tiles or until 10 hours of simulated time; shaded regions show 90% range of growth rates. Nucleation rate simulations used Rgrow's FFS implementation for flat assemblies.

to analyse: growth can proceed entirely by pathways with two-bond attachments, and the growth front for two-bond attachments remains approximately of constant size. Rgrow can be set to flat or tube simulations; in simulations set for tube assemblies, rgrow treats the tube topology and circumference as a fixed property of the assembly, not allowing for tubes of different circumference, or a 2D lattice. Regardless of its topology, the assembly begins from an initial seed assembly which can be specified at the start of the simulation.

4.1 Simulations, and comparison with theory

For comparisons between kBlock simulations and our theoretical analysis, we used a simple 12-tile system forming a periodic 12-helix tube (Figure 3(a)). Every glue was defined to have an identical strength, with $\Delta G(37\,^\circ\mathrm{C}) = -10.15\,\mathrm{kcal\,mol^{-1}}$ and $\Delta S = 193.9\,\mathrm{cal\,mol^{-1}\,K^{-1}}$ (from the representative sequence `TGTCTTGTCA`). Growth rates for tubes used no adjustable parameter other than the growth frontier size parameter $\gamma = 3.5$ (see Section 3.1), set for a 12-helix tube with 0 to 6 two-bond attachment and detachment sites during kBlock_2 growth.

Nucleation rate estimates in simulations used the forward-flux-sampling (FFS) implementation in Rgrow [7, 1]. Application of the theoretical nucleation rate analysis, however, required an estimate of the critical nuclei. To simplify the analysis, nucleation simulations used a flat plane, rather than tube, effectively making the system a 2D periodic lattice. The critical nucleus size was then estimated by taking the maximum critical nucleus assembly free energy along a pathway of increasing $k \times k$ and $k \times (k+1)$ rectangular assemblies. Additionally, classical nucleation theory as applied to tile assembly [22] primarily calculates an upper bound, often orders of magnitude higher than observed nucleation rates (either in simulation or experiments), and is primarily used to consider scaling of nucleation rates when varying parameters. To consider this scaling, for Figure 3, we scaled the theoretical rate to be equal to the simulation rate at 46 °C when varying temperature, and to the simulation rate at 20× blocker concentration when varying blocker concentration.

Simulations: growth

Figure 3 shows simulation results with varying temperature and blocker concentration. In general, simulations align with theory near the two-bond melting point. Unlike the simulations, the theoretical growth rate (dashed curve) assumes that growth occurs only by two-bond attachments, leveraging the assumption that one-bond attachments are too unfavourable to be significant. As temperature decreases, and bond strength thus increases, one-bond attachments may become favourable, with different kinetics and the possibility of a changing growth front size; this would be expected to increase the observed growth rate compared to the theoretical two-bond rate, as seen in simulations at low blocker concentrations. However, at sufficiently high blocker concentrations, even at low temperatures, simulated growth rate remains near the two-bond rate, suggesting that blockers may reduce one-bond attachment pathways, and potentially disordered growth, at low temperatures. For blocker concentrations above 5×, where theory and simulation agree well, as blocker concentrations increase, the growth rate decreases, but slowly at optimal growth temperatures. Both the maximum temperature with a positive growth rate, and the temperature of maximum growth rate, decrease, but only very slightly with increasing blocker concentration, going from 46.0 °C at 5× blocker concentration to 46.8 °C at 40× blocker concentration. Growth occurs only in an increasingly narrow temperature range, going from a full-width-half-max of 8.6 °C at 5× blocker concentration to 4.1 °C at 40× blocker concentration.

Simulations: nucleation

For nucleation, the scaling of nucleation rates at high temperatures, varying blocker concentration, largely fits the theoretical analysis, particularly when moving closer to the melting temperature. At lower temperatures and low blocker concentrations, however, the scaling of the FFS-calculated nucleation rate diverges significantly from the theoretical estimate. It is likely that in these conditions, our simple assumption of an increasing-size-rectangle pathway breaks down, as single-bond attachments may not be significantly unfavourable, or may be even be favourable (eg, below 36.0 °C for 0× blocker concentration). It is also possible that in these conditions, the classical nucleation theory assumption of nucleation rates being constrained by a maximally-unfavourable critical nucleus may break down.

Simulations: tile buffering

As predicted in Remark 18, simulations show a "buffering" effect, where for a particular target initial growth rate, systems with blockers decrease in growth rate more gradually than a system without blockers that starts with a similar growth rate: while a system in the kBlock model will have the growth rate of an equivalent kTAM system with effective tile concentration $p_a c_t$, as tiles are incorporated into assemblies, and c_t decreases, the reduction in growth rate will be slower if $p_a < 1$. Practically, for high blocker concentrations, where p_a does not depend on c_t, this gives a constant multiplicative reduction in the change in growth rate, depending on p_a, which can be influenced by temperature and blocker concentration.

Figure 4 gives an example of how this effect might be applied. Starting from a base 25 nM tile concentration, 12-tile-tube system without blockers, at a fixed temperature, systems with higher tile concentrations can be made to matching initial growth rate by adding a calculated concentration of blockers. Though they grow similarly at first, these systems will continue to grow even when significantly more tiles have been incorporated into assemblies.

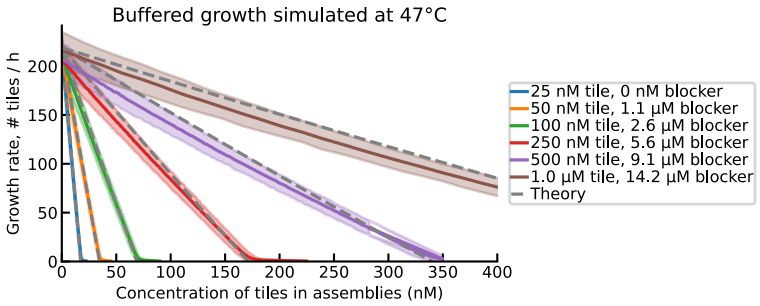

Figure 4 The growth rates of a simple twelve-tile tube system under varying tile and blocker concentrations, representing behaviour when free tiles have been depleted by growth. Solid lines represent simulated results from 1,024 simulated assemblies grown to a size of 1,200 tiles or until 10 hours of simulated time elapsed (shaded regions show 90% range of growth rates), while dashed curves indicate theoretical predictions. All simulations were seeded, with initial blocker concentrations adjusted such that all systems have the same initial growth rate.

4.2 Comparisons between simulation and experimental implementations

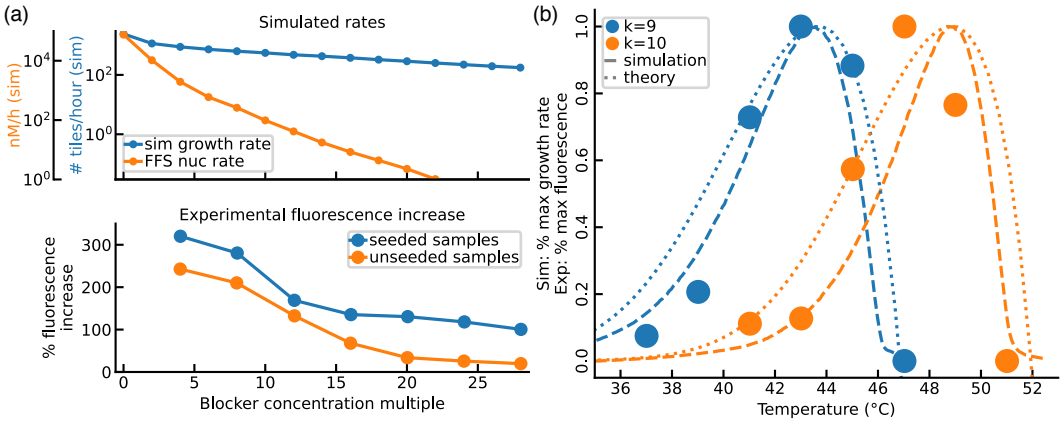

Figure 5 (a) Simulated and experimental results from a twelve-helix tube system. Simulated results show growth rates for a single assembly and spontaneous nucleation rates, without considering depletion. Experimental results measure total growth of assemblies, both from seeds and through spontaneous nucleation, over 96 hours. (b) Simulated, theory and experimental seeded growth results from multiple systems with different glue strengths. Dots show increase in fluorescence (experiment). Dashed line shows mean simulated growth rate from 1,024 simulated assemblies. Dotted line shows theoretical growth rate, assuming all bonds have strength equal to the mean bond strength of the simulated system. Curves are scaled from minimum (or zero, for the theoretical growth rate) to maximum values within the plotted temperature range.

In the first series of experiments, Rogers et al. [17, 18] used a periodic 12-helix DNA tile nanotube system similar to the system used for comparisons between simulations and theoretical values, though for comparison, simulations use sequence-dependent nearest-neighbour energies to reflect the experimental system. Both seeded and spontaneously nucleated tubes were grown. Seeds were purpose-designed 12-helix DNA origami barrels. Tubes were grown in a series of temperature holds, using a qPCR machine repurposed to measure fluorescence under a programmable temperature protocol. The experimental implementations measured growth by a fluorescent reporter mechanism that periodically incorporated Forster resonance energy transfer (FRET) pairs into growing tubes, resulting

in an increase in bulk fluorescence corresponding to tube growth. Experimental data is in Figure 5. Each data point in Figure 5(a) is the maximum, over 6 temperatures (43–53°C in 2°C increments), of the measured fluorescence increase after a 96-hour temperature hold [17]. Figure 5(b) shows measured fluorescence increase after a 48-hour temperature hold from [18].

Growth rate: Simulation versus experiment

For seeded experiments, with fixed seed count and no unseeded nucleation, fluorescence increase over time is a measure of the experimental growth rate. In Figure 5(a), we qualitatively compare maximum growth (via fluorescence increase) across temperatures for the experimental system, both when seeded and unseeded – in which case growth required spontaneous nucleation. Despite mixing system behaviours across a wide range of temperatures, and not accounting for tile depletion in simulations, simulations show a mild and decreasing decline in growth rates with increasing blocker concentration, as is also seen experimentally. A nucleation rate that is very high is also seen (and thus would be depletion-limited) for blocker concentrations where significant increases in fluorescence were observed in unseeded samples, exponentially decreasing across the range of blocker concentrations to be below ranges, per FFS predictions, likely matching minimal experimental nucleation.

Multiple bond strengths: Simulation versus experiment

In a second series of experiments, Rogers et al. implemented multiple 12-helix tube systems, each with glues of different DNA domain lengths, and thus binding strengths, and measured the growth of these systems with fixed blocker concentrations. We consider primarily the growth rate of these systems when seeded. Complexities of fluorescent reporting, however, meant that these were not expected to be measures of absolute growth rate across different tile systems: rather, the increase in fluorescence, for each system separately, was used as a relative measure of growth rate when comparing growth at different temperatures. Our comparison, in Figure 5, thus uses the increase in fluorescence scaled from the minimum increase for each system (always at a temperature above the melting temperature for the system), to the maximum increase within the temperature range. Our simulated growth rate is scaled similarly, while our theoretical growth rate is scaled between the theoretical zero growth rate and the maximum within the range, as the theoretical rate includes negative rates for melting of existing structures at high temperatures, which was not possible in simulations or experiments starting from seeds. As the theoretical two-bond growth rate is for systems with equal bond strengths, the mean bond strength for each system was used.

Simulation closely match experimental temperatures in the multi-system case, especially considering the paucity of experimental temperature points. The temperature of maximum growth rate in simulation is between the highest two experimental growth rate temperatures for all systems, and the full-width-half-max temperature window is comparable, smaller in simulations by 9.8 % for $k = 9$ and 11.7 % for $k = 10$. This close agreement of temperature window size motivates the omission of partially-blocked attachment events in the model: as discussed in Section B, the inclusion of partially-blocked attachment rates results in a significantly wider temperature window than seen experimentally, with a shallower fall-off in rates at low temperatures. Theoretical growth rate estimates, while matching the simulated temperatures of maximum growth rate, have a wider temperature window. As the theoretical estimate uses the mean bond strength, this result is expected: compared to the equal bond strength case, the weakest tile-assembly bonds will reduce growth at high temperatures, and the strongest cover-tile bonds will reduce growth at low temperatures.

5 Discussion

Despite the simplicity of our models, both theoretical analysis and simulations fit experiments well. That they do so despite disallowed reactions is perhaps unexpected. Remark 10 describes physically-plausible phenomena that may result in these reaction pathways being rare, but further analysis and experimental investigation would be fruitful. Nevertheless the simple model seems to provide a good approximation of experimental behaviours. The model, theoretical tools and simulations may be predictive of blocker systems beyond the tile systems studied here, and are likely applicable to a wider range of tile motifs.

Our model predicts that, with sufficient blocker concentration, both growth and spontaneous nucleation will be possible only within a fixed temperature window and both will have maximum rates at particular temperatures. If the maximum rate of spontaneous nucleation is low, then no matter how low the temperature is spontaneous nucleation will not be significant, unlike the no-blocker scenario where nucleation rates are very high at low temperatures. Similarly, below the temperature window for growth, growth will not occur: unlike tile assembly without blockers, where lower temperatures lead to disordered growth, with sufficient blockers, no growth will take place at all. While these results are in a model that does not consider non-lattice interactions that could be viable at low temperature, intuitively, they are based on simple tile-blocker dimerization that should continue to be relevant at low temperatures. Such temperature-dependent behaviour offers several possibilities. For example, could temperature be used as a programmable, time-dependent input to the growth of structures? Could ordered assemblies be grown without a typical high-to-low temperature annealing protocol, instead starting at room temperature, below the growth temperature window, and then simply heating the system to a viable growth temperature? We intentionally model only simple blockers in our model, to match those used in experiments. Numerous variations could have potentially interesting behaviours, especially if combined. Increasing and decreasing the strength of blocker glues compared to tile glues (for example, by making them longer or shorter than the binding regions) could be a stronger mechanism for tuning effective tile concentration than blocker concentration alone, potentially avoiding the need for large blocker concentrations. Multiple-edge blockers could have different, perhaps even error-reducing, properties, incorporating cooperative attachment into the blocker mechanism. We also have not yet explored the effect of blockers on algorithmic self-assembly, where it could change error rate properties.

More generally, our work provides a kinetic explanation for a tile assembly mechanism beyond the colder-is-faster dynamics of passive tile self-assembly, through addition of simple reactions interfering with/mediating the self-assembly process. What other forms of "modified kinetics" might exist, and what behaviours could they exhibit? Could modifications allow for new tradeoffs, e.g. speed-accuracy tradeoff in algorithmic kTAM self-assembly, or other error reduction mechanisms entirely? Could they offer resilience to temperature, energy or concentration variability? Do such simple mediating self-assembly reactions exist in nature?

References

1 Rosalind J. Allen, Chantal Valeriani, and Pieter Rein ten Wolde. Forward flux sampling for rare event simulations. *Journal of Physics: Condensed Matter*, 21(46):463102, October 2009. doi:10.1088/0953-8984/21/46/463102.

2 Robert D. Barish, Paul W. K. Rothemund, and Erik Winfree. Two Computational Primitives for Algorithmic Self-Assembly: Copying and Counting. *Nano Letters*, 5(12):2586–2592, December 2005. doi:10.1021/nl0520381.

3 Robert M. Dirks, Justin S. Bois, Joseph M. Schaeffer, Erik Winfree, and Niles A. Pierce. Thermodynamic Analysis of Interacting Nucleic Acid Strands. *SIAM Review*, 49(1):65–88, January 2007. doi:10.1137/060651100.

4 David Doty. Theory of algorithmic self-assembly. *Communications of the ACM*, 55(12):78–88, December 2012. doi:10.1145/2380656.2380675.

5 Phillip Drake, Daniel Hader, and Matthew J. Patitz. Simulation of the Abstract Tile Assembly Model Using Crisscross Slats. In Shinnosuke Seki and Jaimie Marie Stewart, editors, *30th International Conference on DNA Computing and Molecular Programming (DNA 30)*, volume 314 of *Leibniz International Proceedings in Informatics (LIPIcs)*, pages 3:1–3:25, Dagstuhl, Germany, 2024. Schloss Dagstuhl – Leibniz-Zentrum für Informatik. doi:10.4230/LIPIcs.DNA.30.3.

6 Constantine Evans. *Crystals That Count!* PhD thesis, California Institute of Technology, Pasadena, CA, USA, 2014.

7 Constantine Evans, Jackson O'Brien, Damien Woods, Erik Winfree, and Arvind Murugan. Controlling kinetic pathways in self-assembly through subtle concentration patterns. In preparation.

8 Constantine Evans and Angel Cervera Roldan. Rgrow tile assembly simulator, April 2025. doi:10.5281/zenodo.15232767.

9 Constantine Evans and Erik Winfree. Physical principles for DNA tile self-assembly. *Chemical Society Reviews*, 46(12):3808–3829, 2017. doi:10.1039/C6CS00745G.

10 Constantine Glen Evans, Jackson O'Brien, Erik Winfree, and Arvind Murugan. Pattern recognition in the nucleation kinetics of non-equilibrium self-assembly. *Nature*, 625(7995):500–507, January 2024. doi:10.1038/s41586-023-06890-z.

11 Pedro Fonseca, Flavio Romano, John S. Schreck, Thomas E. Ouldridge, Jonathan P. K. Doye, and Ard A. Louis. Multi-scale coarse-graining for the study of assembly pathways in DNA-brick self-assembly. *The Journal of Chemical Physics*, 148(13):134910, April 2018. doi:10.1063/1.5019344.

12 Shuoxing Jiang, Fan Hong, Huiyu Hu, Hao Yan, and Yan Liu. Understanding the Elementary Steps in DNA Tile-Based Self-Assembly. *ACS Nano*, 11(9):9370–9381, September 2017. doi:10.1021/acsnano.7b04845.

13 Yonggang Ke, Luvena L. Ong, William M. Shih, and Peng Yin. Three-Dimensional Structures Self-Assembled from DNA Bricks. *Science*, 338(6111):1177–1183, November 2012. doi:10.1126/science.1227268.

14 L D Landau and E M Lifshitz. *Statistical Physics*, volume 5. Pergamon Press, 2 edition, 1970.

15 Dionis Minev, Christopher M. Wintersinger, Anastasia Ershova, and William M. Shih. Robust nucleation control via crisscross polymerization of highly coordinated DNA slats. *Nature Communications*, 12(1):1741, March 2021. doi:10.1038/s41467-021-21755-7.

16 Matthew J. Patitz. An introduction to tile-based self-assembly and a survey of recent results. *Natural Computing*, 13(2):195–224, June 2014. doi:10.1007/s11047-013-9379-4.

17 Trent Rogers, Constantine Evans, and Damien Woods. Covered DNA core tiles for robust tuning of spurious nucleation. *DNA28*, 2022. (conference talk, full paper in preparation).

18 Trent Rogers, Constantine Evans, and Damien Woods. A 1D nanoscale printer: assembling DNA nanotubes of arbitrary and precise length from a fixed DNA tile set. *DNA30*, 2024. (conference talk, full paper in preparation).

19 John SantaLucia. A unified view of polymer, dumbbell, and oligonucleotide DNA nearest-neighbor thermodynamics. *Proceedings of the National Academy of Sciences*, 95(4):1460–1465, February 1998. doi:10.1073/pnas.95.4.1460.

20 Samuel W. Schaffter, Dominic Scalise, Terence M. Murphy, Anusha Patel, and Rebecca Schulman. Feedback regulation of crystal growth by buffering monomer concentration. *Nature Communications*, 11(1):6057, November 2020. doi:10.1038/s41467-020-19882-8.

21 Rebecca Schulman and Erik Winfree. Synthesis of crystals with a programmable kinetic barrier to nucleation. *Proceedings of the National Academy of Sciences*, 104(39):15236–15241, September 2007. doi:10.1073/pnas.0701467104.

22 Rebecca Schulman and Erik Winfree. Programmable Control of Nucleation for Algorithmic Self-Assembly. *SIAM Journal on Computing*, 39(4):1581–1616, January 2010. doi:10.1137/070680266.

23 Bryan Wei, Mingjie Dai, and Peng Yin. Complex shapes self-assembled from single-stranded DNA tiles. *Nature*, 485(7400):623–626, May 2012. doi:10.1038/nature11075.

24 Erik Winfree. Simulations of Computing by Self-Assembly. Caltech Technical Report CS-TR:1998.22, Caltech, 1998.

25 Christopher M. Wintersinger, Dionis Minev, Anastasia Ershova, Hiroshi M. Sasaki, Gokul Gowri, Jonathan F. Berengut, F. Eduardo Corea-Dilbert, Peng Yin, and William M. Shih. Multi-micron crisscross structures grown from DNA-origami slats. *Nature Nanotechnology*, 18(3):281–289, March 2023. doi:10.1038/s41565-022-01283-1.

26 Damien Woods, David Doty, Cameron Myhrvold, Joy Hui, Felix Zhou, Peng Yin, and Erik Winfree. Diverse and robust molecular algorithms using reprogrammable DNA self-assembly. *Nature*, 567(7748):366–372, March 2019. doi:10.1038/s41586-019-1014-9.

A A unitful-energy reparametrization of the kTAM

For comparisons to the kTAM model [24, 9], we use a reparametrization of the kTAM in terms of unitful energies, rather than dimensionless, sign-reversed energies. In the reparametrized model, the governing rate equations are

$$r_{\text{att}} = k_{\text{f}} c_{\text{t}} \qquad r_{\text{det}} = k_{\text{f}} e^{\beta b \Delta G_{\text{bond}}(T) - (b-1)\Delta S_{\text{lat}}/R} \tag{10}$$

These parameters are related to the dimensionless kTAM [24, 9] as:

$$c_{\text{t}} = e^{-G_{\text{mc}}+\alpha} \qquad \Delta G_{\text{bond}}(T) = -RT(G_{\text{se}} - \alpha) \qquad \Delta S_{\text{lat}} = R\alpha \tag{11}$$

$$G_{\text{mc}} = \alpha - \ln c_{\text{t}} \qquad G_{\text{se}} = -\beta \Delta G_{\text{bond}}(T) + \alpha \qquad \alpha = \Delta S_{\text{lat}}/R \tag{12}$$

It is easily seen that the kBlock model, with $c_{\mathfrak{b}} = 0$ and $p_{\text{a}} = 1$, is equivalent to this parametrization of the kTAM.

B Partially-blocked attachment events

In the kBlock model, we make the assumption that a tile state may only attach if the tile would not be adjacent to any edge of any tile state in the assembly with a bound blocker. It is possible, and perhaps even more physically plausible, to consider the model where the opposite choice is made: where a tile can attach if there is at least one edge where it can make a bond, regardless of blockers on other edges. We will refer to this model as the kBlockP, where "P" stands for partial binding. Rates will remain the same: the only significant difference is that now, there may be blockers blocking bonds between adjacent tiles in an assembly. We will assume that these bonds are not able to form with the blocker present, but that those blockers will detach with the same rate as blockers elsewhere, and that when they do, the adjoining tiles will immediately make a bond if they have complementary glues on those edges, changing their detachment rates.

The kBlockP model does not satisfy detailed balance: there is no blocker attachment reaction corresponding to a blocker detaching from a position where there is a neighbouring tile. Like the kTAM, the blocker model treats reactions at a tile (and blocker) level as being single steps, rather than considering the attachment and detachment of individual bonds

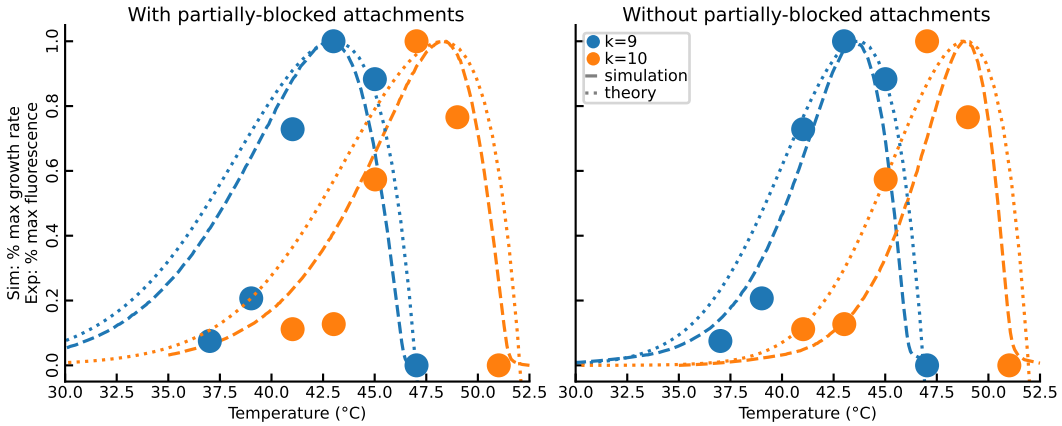

Figure 6 Comparison of growth rates. **Left**: With partially-blocked attachment events, i.e. using the kBlockP$_2$ model discussed here in Section B. **Right**: Without partially-blocked attachment events, i.e. using the kBlock$_2$ model defined in Definition 12.

as the elementary reactions. This approach is considerably simpler and easier to consider physically-realistic parameters for: it is not clear, for example, what the kinetics of individual bond formation and breakage would be. However, for reaction pathways where individual bond formation and breakage must be considered, such models either violate detailed balance, if only one reaction direction can be included, as is the case here and with fission reactions in many kTAM implementations, or omit reaction pathways entirely, for example, for the fission of a 1D line of tiles, where the kTAM would calculate the line breaking in two based on tiles attached by two bonds, whereas a bond-level model would allow the line to break by the much faster reaction of only a single bond breaking. For the kBlockP model, we expect the omitted reaction pathways would be sufficiently rare, and the violation of detailed balance sufficiently small, so as to not significantly affect simulation results. However, a more general bond-based model, with or without blockers, is an open area for future work.

A similar kBlockP$_2$ can be developed, but in this case, we will allow attachments by two bonds, or by tiles that could form two bonds, but have one bond blocked. Similar theoretical results can then be shown, primarily that kBlockP$_2$ will have the same two-bond growth rate as a kTAM$_2$ system with the effective tile concentration of $c_{\text{kTAM}} = p_{\text{a}} c_{\text{kBlock}}$, rather than $p_{\text{a}}^2 c_{\text{kBlock}}$, and that nucleation rates through a critical nucleus with N tiles and B bonds will be reduced by a factor of p_{a}^B. These results also fit simulation results well, when the simulation uses the kBlockP$_2$ model.

However, in comparison to experimental results for multiple systems of varying bond strengths, shown in Figure 6, the temperature dependence of the kBlockP growth rate is significantly different from the experimental results, compared to the kBlock model, which matches surprisingly well.